Available online at www.derpharmachemica.com

ISSN 0975-413X
CODEN (USA): PCHHAX

Der Pharma Chemica, 2016, 8(2):422-433
(http://derpharmachemica.com/archive.html)

Investigation of (4Z)-4-(*2H*-1,4-benzothiazin-3(4H)-ylidene)-5-methyl-2-phenyl-2,4-dihydro-3H-pyrazol-3-one as a new corrosion inhibitors in molar hydrochloric acid: Computational calculations

I. Chakib[1], H. Elmsellem[2], N. K. Sebbar[1], E. M. Essassi[1], I. Fichtali[3], A. Zerzouf[4], Y. Ouzidan[3], A. Aouniti[2], B. El Mahi[2] and B. Hammouti[2]

[1]*Laboratoire de Chimie Organique Hétérocyclique, URAC 21, Pôle de Compétences Pharmacochimie, Université Mohammed V, Faculté des Sciences, Av. Ibn Battouta, Rabat, Morocco*
[2]*Laboratoire de Chimie Appliquée et environnement (LCAE-URAC18), Faculté des Sciences, Oujda, Morocco*
[3]*Laboratoire de Chimie Organique Appliquée, Université Sidi Mohamed Ben Abdallah, Faculté des Sciences et Techniques, Route d'Immouzzer, Fès, Morocco*
[4]*Laboratoire de Chimie Organique et Etudes Physicochimiques, ENS Takaddoum, Université Mohammed V, Rabat, Morocco*

ABSTRACT

The purpose of this study was to examine the effect of (4Z)-4-(2H-1,4-benzothiazin-3(4H)-ylidene)-5-methyl-2-phenyl-2,4-dihydro-3H-pyrazol-3-one ***(P1)*** *as a corrosion inhibitor on mild steel in 1M HCl solution using the weight loss, the potentiodynamic polarization and electrochemical impedance spectroscopy (EIS) techniques. The efficiency of inhibition of each inhibitor increases with increasing of inhibitor concentration at 308K, which leads to a significant reduction in the corrosion rate of mild steel. The adsorption of (4Z)-4-(2H-1,4-benzothiazin-3(4H)-ylidene)-5-methyl-2-phenyl-2,4-dihydro-3H-pyrazol-3-one* ***(P1)*** *on the surface of the mild steel has been well described by the Langmuir adsorption model and quantum chemical calculations were carried out to establish the mechanism of corrosion inhibition.*

Key words: 1,4-benzothiazine, Pyrazolone, Mild steel, Electrochemical methods, 1M HCl , DFT.

INTRODUCTION

[1,4]-benzothiazines derivatives have constituted an important class of heterocyclic compounds which, even when part of a complex molecule [1], possess a wide spectrum of biological activities [2-4], due to the presence of a fold along the nitrogen sulfur axis. The biological activity of some [1,4]-benzothiazines derivatives is similar to that of phenothiazines, featuring the same structural specificity [5-9]. The role of [1,4]-benzothiazine in medicinal chemistry was reviewed earlier [10]. Generally, benzothiazine and derivatives have found widespread application as analgesic [11-12], antibacterial [13-14], anticancer [15], anticonvulsant [16], anthelmintic [17]. These properties indicate that [1,4]-benzothiazine is a template that may be potentially useful in medicinal chemistry research and therapeutic applications. Furthermore pyrazole derivatives occupy an important position in medicinal chemistry due to their wide range of bioactivities such as anticancer [18], anticonvulsant [19], antimalarial [20], etc.

The present study aimed to test new compound named (4Z)-4-(2H-1,4-benzothiazin-3(4H)-ylidene)-5-methyl-2-phenyl-2,4-dihydro-3H-pyrazol-3-one **(P1)** on the corrosion of mild steel in 1 M hydrochloric acid solution. In this work, we are interested in the synthesis of the title compound for biological activities, [21-22] by condensation dithiodianiline and 5-[1-phenyl-3-methyl-5-oxo-pyrazol-4-ylidene]-1.7-dimethyl-3-phénylpyrano[2,3-c]pyrazole, in

n-butanol The resulting major product was precipitated in n-butanol then filtered and recrystallized from dichloromethane **Scheme 1**.

In continuation of our work on development of 1,4-benzothiazine derivatives as corrosion inhibitors in acidic environment [23-38], we have studied the inhibiting effect of (4Z)-4-(2H-1,4-benzothiazin-3(4H)-ylidene)-5-methyl-2-phenyl-2,4-dihydro-3H-pyrazol-3-one **(P1)** on the corrosion of mild steel in 1 M HCl using polarization measurements, impedance techniques, weight loss measurements and quantum chemical calculations. The relationship between calculated quantum chemical parameters and experimental inhibition efficiencies of the inhibitors was discussed.

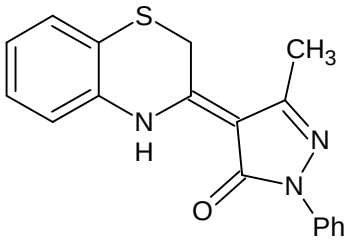

Scheme 1: (4Z)-4-(2H-1,4-benzothiazin-3(4H)-ylidene)-5-methyl-2-phenyl-2,4-dihydro-3H-pyrazol-3-one (P1)

MATERIALS AND METHODS

2.1. Materials and sample preparation

The composition (wt.%) of mild steel samples used for all the experiments was as follows: C = 0.253; Si = 0.12; P = 0.013; S = 0.024; Cr = 0.012; Mn = 0.03 and balance Fe. Coupons cut into 1.5 x 1.5 x 0.05 cm size were used for gravimetric measurements whereas specimens of size with 1 cm^2 exposed surface areas were used as working electrode for polarization and EIS measurements. Before starting the experiments, the specimens were mechanically abraded with 320, 400, 600, 800, 1000 and 1200 grade of emery papers. These were then degreased with acetone, washed with double distilled water and dried in air before immersing in the corrosive medium.

The corrosive solution, 1.0 M HCl was prepared by dilution of analytical grade HCl of predetermined normality with triple distilled water. The concentration range of P1 used was 10^{-6} M to 10^{-3} M. The volume of electrolyte used in each experiment was 100 mL.

2.2. Synthesis of inhibitors

To a solution of 5-[1-phenyl-3-methyl-5-oxo-pyrazol-4-ylidene]-1.7-dimethyl-3-phénylpyrano[2,3-c]pyrazole (0.0025 mole) in n-butanol (60 mL) and was added (0.004 mole) of dithiodianiline. The resulting reaction mixture was stirred at refluxed for 72 h and major product was precipitate in n-butanol, was obtained in a yield 65% and recrystallized from dichloromethane (M.p 434-436 K) **Scheme 2**.

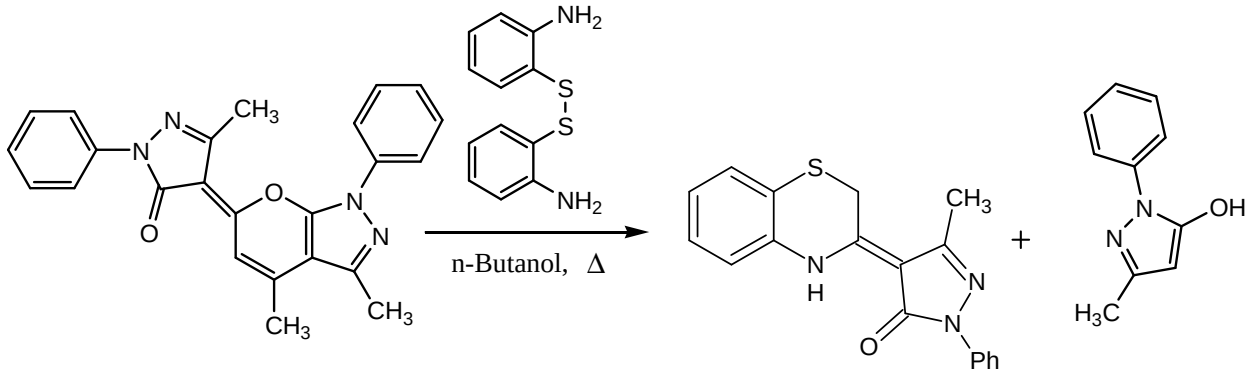

Scheme 2: Synthesis of (4Z)-4-(2H-1,4-benzothiazin-3(4H)-ylidene)-5-methyl-2-phenyl-2,4-dihydro-3H-pyrazol-3-one (P1)

The analytical and spectroscopic data are conforming to the structure of compound (4Z)-4-(2H-1,4-benzothiazin-3(4H)-ylidene)-5-methyl-2-phenyl-2,4-dihydro-3H-pyrazol-3-one **(P1)** formed.

(P1):**Yield =** 65%; **M.p.** 434-436 K; **RMN1H (DMSO-d6) δ ppm :** 2.5 (s, 3 H, CH_3), 3.4 (s, 2H, S-CH_2), 7.36-8.09 (m, 7H, CHar); **RMN13C (DMSO-d6) δ ppm :** 12.99 (CH_3), 37.854 (CH_2), 163.59 (C=O), 159.617 ; 155.514,

152.647 ; 134.266, 133.801, 104.937 (Cq), 129.940, 128.307 ; 126.540 ; 125.527 ;124.814 ; 122.335 ; 122.162 (CH ar).

2.3. Experimental techniques

2.3.1. Weight loss measurements

Coupons were cut into 1.5× 1.5 × 0.05 cm^3 dimensions having composition (0.09 % P, 0.01 % Al, 0.38 % Si, 0.05 % Mn, 0.21 % C, 0.05 % S and Fe balance) used for weight loss measurements. Prior to all measurements, the exposed area was mechanically abraded with 180, 400, 800, 1000, 1200 grades of emery papers. The specimens are washed thoroughly with bidistilled water degreased and dried with ethanol. Gravimetric measurements are carried out in a double walled glass cell equipped with a thermostated cooling condenser. The solution volume is 100 cm^3. The immersion time for the weight loss is 6 h at (308±1) K. In order to get good reproducibility, experiments were carried out in duplicate. The average weight loss was obtained. The corrosion rate (**v**) is calculated using the following equation:

$$\mathbf{v = W / S.}t \qquad \textbf{(1)}$$

Where W is the average weight loss, S the total area, and t is immersion time. With the corrosion rate calculated, the inhibition efficiency (Ew) is determined as follows:

$$\mathrm{Ew}\,\% = \frac{V0-V}{V0}\ \mathrm{X}\ 100 \qquad \textbf{(2)}$$

Where $\mathbf{V_0}$ and **V** are the values of corrosion rate without and with inhibitor, respectively.

2.3.2. Electrochemical tests

The electrochemical study was carried out using a potentiostat PGZ100 piloted by Voltamaster soft-ware. This potentiostat is connected to a cell with three electrode thermostats with double wall. A saturated calomel electrode (SCE) and platinum electrode were used as reference and auxiliary electrodes, respectively. Anodic and cathodic potentiodynamic polarization curves were plotted at a polarization scan rate of 0.5mV/s. Before all experiments, the potential was stabilized at free potential during 30 min. The polarisation curves are obtained from −800 mV to −200 mV at 308 K. The solution test is there after de-aerated by bubbling nitrogen. Inhibition efficiency (Ep%) is defined as Equation3, where icorr(0) and icorr(inh) represent corrosion current density values without and with inhibitor, respectively.

$$Ep\% = \frac{\mathrm{icor(0)-icor(inh)}}{\mathrm{icor(0)}}\ \mathrm{x}\ 100 \qquad \textbf{(3)}$$

The electrochemical impedance spectroscopy (EIS) measurements are carried out with the electrochemical system, which included a digital potentiostat model Voltalab PGZ100 computer at Ecorr after immersion in solution without bubbling. After the determination of steady-state current at a corrosion potential, sine wave voltage (10 mV) peak to peak, at frequencies between 100 kHz and 10 mHz are superimposed on the rest potential. Computer programs automatically controlled the measurements performed at rest potentials after 0.5 hour of exposure at 308 K. The impedance diagrams are given in the Nyquist representation. Inhibition efficiency (E_R%) is estimated using the relation 4, where $R_t(0)$ and Rt(inh) are the charge transfer resistance values in the absence and presence of inhibitor, respectively:

$$ER\% = \frac{\mathrm{Rt(inh)-Rt(0)}}{\mathrm{Rt(inh)}}\mathrm{x}\ 100 \qquad \textbf{(4)}$$

2.4. Computational Details

All quantum chemical study was carried out using the Density Functional Theory (DFT) with hybrid functional B3LYP, based on Becke's three-parameter functional including Hartree–Fock exchange contribution with a nonlocal correction for the exchange potential proposed by Becke [39-40] together with the nonlocal correction for the correlation energy provided by Lee et al. [41]. Since electrochemical corrosion takes place in liquid phase, and for a better approach of the experimental results, we used the Self-Consistent Reaction Field (SCRF) theory [40], with Tomasi's Polarized Continuum Model (PCM) [42], to include the effect of solvent in the computations. This approach models the solvent as a continuum of uniform dielectric constant (ε) and defines the cavity where the solute is placed as a uniform series of interlocking atomic spheres.

The quantum chemical investigations were used to look for good theoretical parameters to be correlated with the inhibitive performance of the studied benzothiazine-pyrazole derivatives. To do so, some of molecular properties, describing the global reactivity such as: the energy of the Highest Occupied Molecular Orbital (E_{HOMO}), the energy of the Lowest Unoccupied Molecular Orbital (E_{LUMO}), the energy gap ($\Delta E=E_{LUMO}-E_{HOMO}$), the electrical dipole moment (μ), the Ionization Potential (IP), the Electron Affinity (EA), the electronegativity (χ) and the global hardness (η) were calculated. Other parameters describing the local selectivity of the studied molecules such as the local natural populations and the Fukui functions were also considered. In order to estimate some of the previous descriptors, the Koopmans' theorem was used [43] to relate the HOMO and LUMO energies to the IP and EA, respectively:

$$IP = -E_{HOMO} \quad \textbf{(5)}$$

$$EA = -E_{LUMO} \quad \textbf{(6)}$$

Then the electronegativity and the global hardness were evaluated, based on the finite difference approximation, as linear combinations of the calculated IP and EA.

$$\chi = \frac{IP + EA}{2} \quad \textbf{(7)}$$

$$\eta = \frac{IP - EA}{2} \quad \textbf{(8)}$$

RESULTS AND DISCUSSION

3.1. Electrochemical measurements

3.1.1. Potentiodynamic polarization studies

Figure 1 shows the typical potentiodynamic polarization curves of mild steel in 1 M HCl solution in the presence and absence of different concentration of P1 at 308K. As can be seen from the figure after addition of inhibitor a decrease in both cathodic and anodic currents was observed, suggesting that the presence of P1 reduced anodic dissolution and also retarded the hydrogen evolution reaction [44-45]. Table 1 shows the electrochemical corrosion kinetic parameters, i.e. corrosion potential (E_{corr}), cathodic and anodic Tafel slopes (βc, βa) and corrosion current density (I_{corr}) obtained from the Tafel extrapolation of the polarization curves. Table 1 also included percentage inhibition efficiency (E_P%).

Table 1. Electrochemical parameters of mild steel in 1M HCl solution without and with P1 at different concentrations

Inhibitor	**Concentration** (M)	**-E_{corr}** (mV/SCE)	**I_{corr}** (μA/cm^2)	**-βc** (μA/cm²)	**Ep** (%)
1M HCl	-	464	1386	184	--
Inhibitor (P1)	10^{-6}	452	239	159	81
	10^{-5}	454	206	173	83
	10^{-4}	459	198	174	85
	10^{-3}	453	157	184	88

Figure 1 shows the potentiodynamic polarization curves of mild steel 1M HCl in the absence and the presence of P1 these potentiodynamic polarization curves illustrate that the presence of our product caused a decrease in both the anodic Tafel and cathodic slope, with a decrease more pronounced in the cathodic branch, demonstrating that this product acts as a mixed inhibitor type with essentially cathodic characteristics.

These results can be explained by the adsorption of organic compounds present in the solution of 1M HCl at the active sites of the electrode surface. While Table 1 shows that the corrosion current density (I_{corr}) decreased in the presence of the inhibitor.

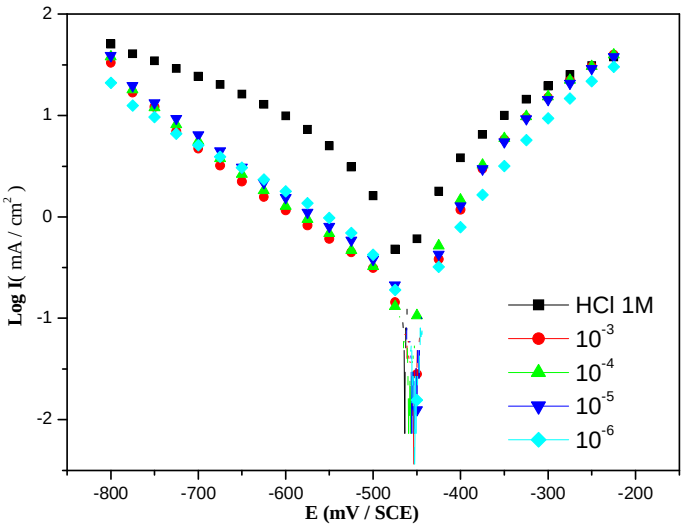

Figure 1. Potentiodynamic polarization curves of mild steel in 1M HCl in the presence of different concentrations of (4Z)-4-(2H-1,4-benzothiazin-3(4H)-ylidene)-5-methyl-2-phenyl-2,4-dihydro-3H-pyrazol-3-one (P1)

3.1.2. Electrochemical Impedance measurements

The impedance measurements were carried out after immersion for 30 min in 1 M HCl solutions in absence and presence of different concentration of (4Z)-4-(2H-1,4-benzothiazin-3(4H)-ylidene)-5-methyl-2-phenyl-2,4-dihydro-3H-pyrazol-3-one **(P1)**. Figure 2 shows typical Nyquist plots for mild steel in 1 M HCl in the absence and presence of studied inhibitor at 308K.

The Nyquist plots show a depressed capacitive loop in the high frequency (HF). The HF capacitive loop can be attributed to the charge transfer reaction and time constant of the electric double layer and to the surface inhomogeneity of structural or interfacial origin, such as those found in adsorption processes [46-47].

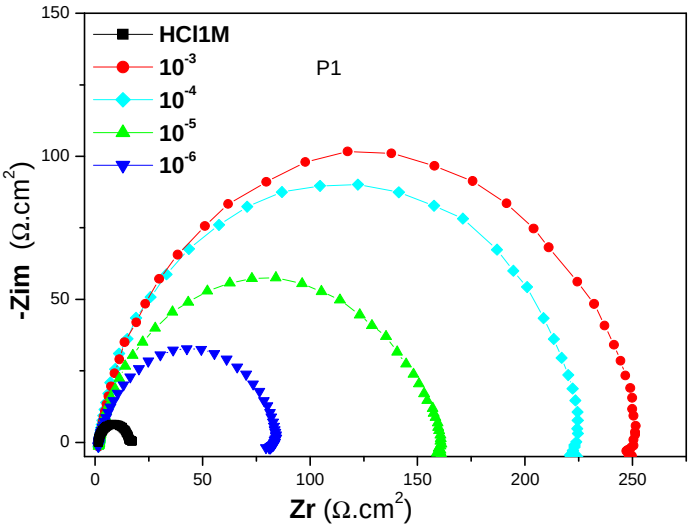

Figure 2. Electrochemical impedance curves of mild steel in 1M HCl without and with different concentrations of (4Z)-4-(2H-1,4-benzothiazin-3(4H)-ylidene)-5-methyl-2-phenyl-2,4-dihydro-3H-pyrazol-3-one (P1)

It was clear that the values of R_{ct} charge transfer resistance has been increased and the capacity C_{dl} values decreased with increasing concentration of inhibitor increased R_{ct} charge transfer resistance is associated with a system slower corrosion.

Table 2. Impedance parameters and inhibition efficiency values for mild steel after 1/2 h immersion period in 1 M HCl containing different concentrations of (4Z)-4-(2H-1,4-benzothiazin-3(4H)-ylidene)-5-methyl-2-phenyl-2,4-dihydro-3H-pyrazol-3-one (P1) at 308 K

Inhibitor	Concentration (M)	R_t ($\Omega.cm^2$)	C_{dl} ($\mu F.cm^{-2}$)	E_{Rt} (%)
1M HCl	-	14.57	200	--
Inhibitor (P1)	$\mathbf{10^{-6}}$	81	63.65	82
	$\mathbf{10^{-5}}$	161	39.29	90
	$\mathbf{10^{-4}}$	225	35.85	93
	$\mathbf{10^{-3}}$	250	32.06	94

Improving the corrosion resistance of mild steel in acid medium results in an increase in charge transfer resistance values could be attributed to adsorption of the inhibitor to the acid-steel interface, which effectively blocked the active sites on the surface of the mild steel and therefore the reduction of C_{dl} values with an increase in the concentration of the inhibitor, suggesting that the thickness of the protective layer increases with decreasing the constant local dielectric [48-50]. Increasing the efficiency of inhibition with increased concentration of the inhibitor promotes increasingly cover the surface of the mild steel with the inhibitor concentrations.

3.2. Weight loss measurements

3.2.1. Effect of inhibitor concentration on corrosion of mild steel

The effect of addition of P1 at various concentrations on the mild steel corrosion in 1 M HCl solution is studied by weight loss measurements at 308K after 6 h immersion. Sometimes the highest concentration is limited by the solubility of the compound. The values of inhibition efficiencies (E_W%) and corrosion rates (w) obtained from weight loss measurements for P1 at different concentrations in 1 M HCl are listed in Table 3. It is found that inhibition efficiency increases with increasing inhibitor concentration, while corrosion rate decreases with inhibitor concentration.

The inhibition of mild steel corrosion can be attributed to the adsorption of the inhibitor at the mild steel/acid solution interface. (4Z)-4-(2H-1,4-benzothiazin-3(4H)-ylidene)-5-methyl-2-phenyl-2,4-dihydro-3H-pyrazol-3-one **(P1)** is good inhibitor showing more than 92% inhibition efficiency at 10^{-3} M concentration. Good performance of (4Z)-4-(2H-1,4-benzothiazin-3(4H)-ylidene)-5-methyl-2-phenyl-2,4-dihydro-3H-pyrazol-3-one **(P1)** as corrosion inhibitors for mild steel in 1 M HCl solutions may be due to the presence of aromatic rings and hetero-atoms in their structures [51].

Percentage inhibition efficiencies obtained from weight loss measurements are comparable and run parallel with those obtained from potentiodynamic polarization and impedance measurements

Table 3. Corrosion parameters obtained from weight loss measurements for mild steel in 1 M HCl containing various concentrations of (4Z)-4-(2H-1,4-benzothiazin-3(4H)-ylidene)-5-methyl-2-phenyl-2,4-dihydro-3H-pyrazol-3-one (P1) at 308 K

Inhibitor	Concentration (M)	W_{corr} ($mg.cm^{-2}.h^{-1}$)	E_w (%)	θ
HCl 1M	--	0.82	--	--
Inhibitor (P1)	$\mathbf{10^{-6}}$	0.12	84	0.84
	$\mathbf{10^{-5}}$	0.09	88	0.88
	$\mathbf{10^{-4}}$	0.06	91	0.91
	$\mathbf{10^{-3}}$	0.05	94	0.94

3.2.2. Adsorption Isotherm

It is well recognised that the first step in inhibition of metallic corrosion is the adsorption of organic inhibitor molecules at the metal/solution interface and that the adsorption depends on the molecule's chemical composition, the temperature and the electrochemical potential at the metal/solution interface. In fact, the solvent H_2O molecules could also adsorb at metal/solution interface.

So the adsorption of organic inhibitor molecules from the aqueous solution can be regarded as a quasi-substitution process between the organic compounds in the aqueous phase [$Org_{(sol)}$] and water molecules at the electrode surface [$H_2O_{(ads)}$] [52].

$$Org_{(sol)} + xH_2O_{(ads)} \longleftrightarrow Org_{(ads)} + xH_2O_{(sol)}$$

Where x is the size ratio, that is, the number of water molecules replaced by one organic inhibitor. Basic information on the interaction between the inhibitor and the mild steel surface can be provided by the adsorption isotherm. In order to obtain the isotherm, the linear relation between degree of surface coverage (θ) values (θ = E%/100; Table 4) and inhibitor concentration (C_{inh}) must be found. Attempts were made to fit the θ values to various isotherms

including Langmuir, Temkin, Frumkin and Flory–Huggins. By far the best fit is obtained with the Langmuir isotherm. This model has also been used for other inhibitor systems [53-54].

According to this isotherm, θ is related to C_{inh} by:

$$\frac{C}{\theta} = \frac{1}{k} + C \qquad \textbf{(9)}$$

Where K_{ads} denotes the equilibrium constant for the adsorption process.

Figure 3 shows the plots of C_{inh}/θ versus C_{inh} and the expected linear relationship is obtained for all compounds.

The strong correlations (R^2 = 0.999 for the compound P1 confirm the validity of this approach. The slopes of the straight lines are 0.904 for P1, suggesting that adsorbed inhibitor molecules form monolayer on the mild steel surface and there is no interaction among the adsorbed inhibitor molecules.

The value of K_{ads} obtained from the Langmuir adsorption isotherm is 7.01 10^5 M^{-1} together with the values of the Gibbs free energy of adsorption $\Delta G°_{ads}$ calculated from the equation:

$$K = \frac{1}{55.55}\exp(-\frac{\Delta G^0_{ads}}{RT}) \qquad \textbf{(10)}$$

Where R is the universal gas constant, T the thermodynamic temperature and the value of 55.5 is the concentration of water in the solution[55].

The high values of K_{ads} for studied P1 indicate stronger adsorption on the mild steel surface in 1 M HCl solution. This can be explained by the presence of hetero-atoms and π-electrons in the inhibitor molecules. The higher the K_{ads} is (7.01 10^5 M^{-1}), the stronger and more stable adsorbed layer is forming, which increases the inhibition efficiency [56].

These data support the good performance (4Z)-4-(2H-1,4-benzothiazin-3(4H)-ylidene)-5-methyl-2-phenyl-2,4-dihydro-3H-pyrazol-3-one **(P1)** as corrosion inhibitor for mild steel in 1 M HCl. The negative values of $\Delta G°_{ads}$, calculated from Eq.(10), are consistent with the spontaneity of the adsorption process and the stability of the adsorbed layer on the carbon steel surface. Generally, the energy values of -20 kJ mol^{-1} or less negative are associated with an electrostatic interaction between charged molecules and charged metal surface, physisorption; those of -40 kJ mol^{-1} or more negative involve charge sharing or transfer from the inhibitor molecules to the metal surface to form a coordinate covalent bond, chemisorption [57]. In present study, the $\Delta G°_{ads}$ values obtained for the (4Z)-4-(2H-1,4-benzothiazin-3(4H)-ylidene)-5-methyl-2-phenyl-2,4-dihydro-3H-pyrazol-3-one **(P1)** on mild steel in 1 M HCl solution is 44.73 kJ mol^{-1}. Therefore, it is concluded that chemical interactions should be dominant for the adsorption of the P1 molecules on the mild steel surface [58].

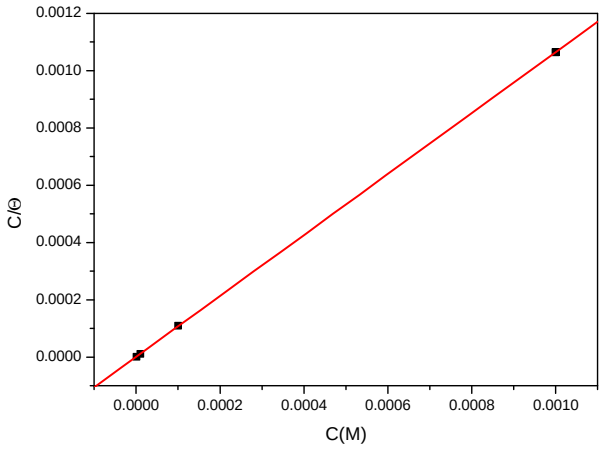

Figure 3. Langmuir adsorption isotherms for P1 at 308K at different concentration in 1 M HCl, obtained from weight loss data

3.3. Molecular geometries

The quantum chemical calculations are performed on an Intel (R) core $(TM)_2$ Quad CPU (2.4 GHz and 8 GB RAM) computer using standard Gaussian-09 software package [59]. The geometries of the pyridine-pyrazole derivatives considered in this work are fully optimized, without any symmetry constraint at DFT level of theory using a B3LYP functional together with 6-31G(d,p) basis set in gaseous phase. Besides, for a better approach of the experimental parameters, the geometries are reoptimized in aqueous phase at the same level of theory using PCM model. The final optimized geometries are given in Figure 4 and the geometrical parameters values are presented in Table 4.

Table 4. Pertinent valence and dihedral angles, in degree, of the studied inhibitors calculated at B3LYP/6-31G(d,p) in gas, G and aqueous, A phases

Angle	Phase	Value
$[C_1C_{22}N_{33}]$	G	120.98188
	A	121.39811
$[C_4N_{15}N_{16}]$	G	118.93685
	A	118.58646
$[C_2C_1C_{22}N_{33}]$	G	0.00176
	A	-0.16025
$[C_6C_4N_{15}N_{16}]$	G	-179.99480
	A	-179.86866

After the analysis of the theoretical results obtained, we can say that the molecule **P2** have a planar structure. In fact, the benzothiazine, pyrazol and benzene rings are circa perpendicular to each other.

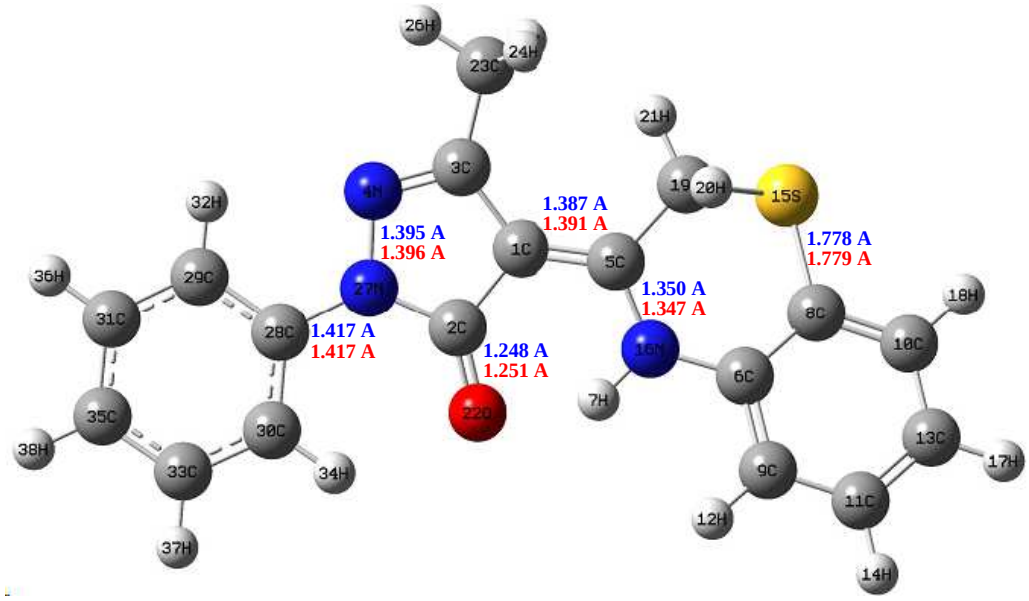

Figure 4. Optimized molecular structures and bond lengths of the studied inhibitors calculated in gas (blue) and aqueous (red) phases at B3LYP/6-31G(d,p) level

phase	TE (eV)	E_{HOMO} (eV)	E_{LUMO} (eV)	ΔE (eV)	μ (D)	IP (eV)	EA (eV)	H (eV)	H (eV)
Gas	-36261.0	-6.1758	-0.0063	6.1695	5.8676	6.1758	0.0063	3.0911	3.0847
Aqueous	-36261.4	-5.5328	-1.8304	3.7014	8.8600	5.5328	1.8304	3. 6816	1.8512

- **Local molecular reactivity**

Besides the global reactivity indicators, the analysis of atoms selectivity within inhibitors is very useful in indicating the reactive sites towards electrophilic and nucleophilic attacks. In the case of an electron-transfer for reaction control, the selectivity descriptors of choice are the condensed Fukui functions on atoms [60]. These descriptors inform about the veritable sites in a molecule on which nucleophilic, electrophilic or radical attacks are most likely possible.

In order to compute the condensed Fukui functions of a system of N electrons, we perform a single point calculation of the anionic (N+1) and the cationic (N-1) species by using the neutral optimized geometry, at the same level of theory. The condensed Fukui functions are then computed using the finite-difference approximation as follow:

$$f_k^+ = P_k(N+1) - P_k(N)$$

$$f_k^- = P_k(N) - P_k(N+1)$$

$$f_k^0 = \frac{P_k(N+1) - P_k(N-1)}{2}$$

where, $P_k(N)$, $P_k(N+1)$ and $P_k(N-1)$ are the natural populations for the atom k in the neutral, anionic and cationic species respectively.

Table 5 and 6 displays the most relevant values of the natural population (P(N), P(N-1) and P(N+1)) with the corresponding values of the Fukui functions (f_k^+, f_k^- and f_k^0) of the studied inhibitors. The calculated values of the f_k^+ for all inhibitors are mostly localized on the pyrazole and benzothiazine ring, namely N_{16}, C_{21}, C_{22}, C_{30} and S_{32}, indicating that the pyrazole and benzothiazine ring will probably be the favorite site for nucleophilic attacks.

The results also show that O_{21} atoms are suitable sites to undergo both nucleophilic and electrophilic attacks, probably allowing them to adsorb easily and strongly on the mild steel surface.

Table 5. Pertinent natural populations and Fukui functions of the studied inhibitors calculated at B3LYP/6-31G(d,p) in gas (G) phase

Atom	Phase	N(K)	N(K+1)	N(K-1)	f_k^+	f_k^-	f_k^0
N_{15}	G	7,2560	7,2614	7,1814	0,0054	0,0746	0,400
N_{16}	G	7,2719	7,3778	7,2364	0,1059	0,0355	0,0707
O_{21}	G	8,6541	8,7142	8,5205	0,0601	0,1336	0,0969
C_{22}	G	5,6849	5,8665	5,6648	0,1816	0,0201	0,1009
C_{30}	G	6,2177	6,3088	6,1936	0,0912	0,0240	0,0576
S_{32}	G	15,3389	15,7507	15,5916	0,4118	-0,2527	0,0796

Table 6. Pertinent natural populations and Fukui functions of the studied inhibitors calculated at B3LYP/6-31G(d,p) in aqueous (A) phase

Atom	Phase	N(K)	N(K+1)	N(K-1)	f_k^+	f_k^-	f_k^0
N_{15}	A	7,2640	7,2665	7,1525	0,0025	0,1115	0,0570
N_{16}	A	7,3105	7,3909	7,2260	0,0804	0,0845	0,0824
O_{21}	A	8,6704	8,7499	8,5284	0,0795	0,1419	0,1107
C_{22}	A	5,6700	5,8537	5,6207	0,1837	0,0493	0,1165
C_{30}	A	6,23914	6,2908	6,20506	0,0517	0,0341	0,0429
S_{32}	A	15,7001	15,8784	15,6521	0,1784	0,0480	0,1132

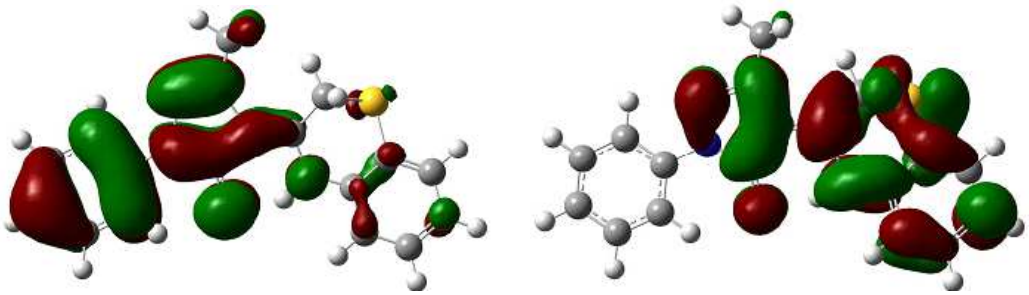

HOMO (G) LUMO (G)

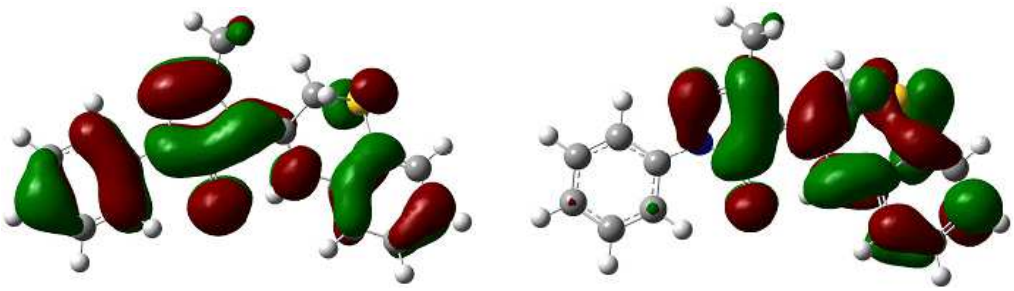

HOMO (A) LUMO (A)

Figure 5. The HOMO and the LUMO electrons density distributions of the studied inhibitors computed at B3LYP/6-31G(d,p) level in gas and aqueous phases

CONCLUSION

❖The (4Z)-4-(2H-1,4-benzothiazin-3(4H)-ylidene)-5-methyl-2-phenyl-2,4-dihydro-3H-pyrazol-3-one **(P1)** show good inhibition properties for the corrosion of mild steel in 1 M HCl solutions and the inhibition efficiency increases with increasing the concentration of the inhibitor.

❖Tafel polarization measurements show that (4Z)-4-(2H-1,4-benzothiazin-3(4H)-ylidene)-5-methyl-2-phenyl-2,4-dihydro-3H-pyrazol-3-one **(P1)** is mixed-type inhibitor. Based on the properties of impedance diagrams (EIS), one equivalent structure model was selected which could fit the experimental data very well.

❖The inhibiting efficiencies obtained by polarization, EIS and weight loss measurements are in good agreement.

❖ The adsorption of (4Z)-4-(2H-1,4-benzothiazin-3(4H)-ylidene)-5-methyl-2-phenyl-2,4-dihydro-3H-pyrazol-3-one **(P1)** on the mild steel/1 M HCl interface obeys the Langmuir adsorption isotherm model.

❖The negative sign of the $\Delta G°_{ads}$ indicate that the adsorption of (4Z)-4-(2H-1,4-benzothiazin-3(4H)-ylidene)-5-methyl-2-phenyl-2,4-dihydro-3H-pyrazol-3-one **(P1)** on the mild steel surface in 1 M HCl is spontaneous. Further the adsorption of **(P1)** on mild steel surface is chemisorption type.

❖ Structural and electronic parameters from the quantum chemical calculations are correlated well to the experimentally obtained inhibition efficiencies.

REFERENCES

[1] R. R Gupta, K. G Ojha, *Chem and Biochemical Aspects, Elsevier, Amsterdam*, **1988**, 4**,** 163-269.
[2] S Gupta, N Ajmera, P Meena, N Gautam, A Kumar, D. C Gautam, *Jordan J. Chem*, **2009**, 4, 209-221.
[3] D Armenise, G Trapani, V Arrivo, E Laraspata, F. Morlacchi, *J. Heterocycl. Chem*, **2000**, 37, 1611–1616.
[4] D Armenise, G Trapani, F Stasi, F Morlacchi, *Arch. Pharm*, **1998**, 331, 54-58.
[5] T. N Bansode, J. V Shelke, V. G Dongre, *Eur. J. Med. Chem*, **2009**, 44, 5094-5098.
[6] Y Dixit, R Dixit, N Gautam, D. C Gautam, *Nucleosides Nucleotides Nucleic Acids*, **2009**, 28, 998-1006.
[7] Y Dixit, R Dixit, N Gautam, D. C Gautam, *E-J. Chem*, **2008**, 5 (S1), 1063-1068.
[8] R. R Gupta, R. S Rathore, M Jain, V Saraswat, *Pharmazie*, **1992**, 47, 229-230.
[9] L Thomas, A Gupta, V Gupta *J. Fluorine Chem*, **2003**, 122, 207-213.
[10] R Fringuelli, L Milanese, F Schiaffella, *Mini-Rev. Med. Chem*, **2005**, 5, 1061-1073.
[11] B. KWarren, E. E Knaus, *Eur. J. Med. Chem*, **1987**, 22, 411- 415.
[12] S. K Dubey, J. M Seda, E. E Knaus *Eur. J. Med. Chem*, **1984**, 19, 371-372.
[13] D Armenise, M Muraglia, M. A Florio, N. D Laurentis, A Rosato, A Carrieri, F Corbo, C Franchini, *Arch. Pharm*, **2012**, 345, 407-416.
[14] S Sabatini, G. W Kaatz, G. M Rossolini, D Brandim, A Fravolini, *J. Med. Chem*, **2008**, 51, 4321-4330.
[15] Y Jacquot, L Bermont, H Giorgi, B. L Refouvelet, G Adessi, E Daubrosse, A Xicluna, *Eur. J. Med. Chem*, **2001**, 36, 127-136.
[16] B Kalluraya, R. M Chimbalkar, J. C Hegde, *Indian J. Heterocycl. Chem*, **2005**, 15, 15-18.
[17] D Munirajasekar, M Himaja, M Sunil, *Int. Res. J. Pharm*, **2011**, 2, 114-117
[18] M.M Ghorab, F.A Ragab, S.I Alqasoumi, A.M Alafeefy, S.A Aboulmagd, *Eur. J. Med. Chem.* **2010**, 45, 171–178.
[19] N.D Amnerkar, K.P Bhusari, *Eur. J. Med. Chem*, **2010**, 45, 149-159.
[20] P.N Kalaria, S.P Satasia, D.K Raval, *New J. Chem.* **2014**, 38, 2902-2910.
[21] N. K. Sebbar, M. Ellouz, E.M. Essassi, Y Ouzidan & J. T. Mague, *Acta Cryst*, **2015**, E71, o999.
[22] M. Ellouz, N.K. Sebbar, E.M. Essassi, Y. Ouzidan, & J. T. Mague, *Acta Cryst*, **2015**, E71, o1022-o1023.
[23] H. Elmsellem, A. Aouniti, M. Khoutoul, A. Chetouani, B. Hammouti, N. Benchat, R.Touzani, M. Elazzouzi, *Journal of Chemical and Pharmaceutical Research*, **2014**, 6(4), 1216-1224.

[24] N. K. Sebbar, H. Elmsellem,M. Ellouz, S. Lahmidi, A.L. Essaghouani, E. M. Essassi, M.Ramdani, A. Aouniti1, B. El Mahi and B. Hammouti. *Der Pharma Chemica*, **2015**, 7(10):579-587.
[25]H. Elmsellem, K. Karrouchi, A. Aouniti, B. Hammouti, S. Radi, J. Taoufik, M. Ansar, M. Dahmani, H. Steli and B. El Mahi, *Der Pharma Chemica*, **2015**,7(10), 237-245.
[26] Zarrouk, B. Hammouti, H. Zarrok, R. Salghi, M. Bouachrine, F. Bentiss, S. S. Al-Deyab, Res Chem Intermed, **2012**, 38 2327.
[27] H. Elmsellem, A. Aouniti, M.H. Youssoufi, H. Bendaha, T. Ben Hadda, A. Chetouani, I. Warad, B. Hammouti, *Phys. Chem. News*, **2013**, 70, 84.
[28] H. Elmsellem, M. H.Youssouf, A. Aouniti, T. Ben Hadd, A. Chetouani, B. Hammouti. Russian, *Journal of Applied Chemistry*, **2014**, 87(6), 744-753.
[29] H. Elmsellem, A. Elyoussfi, H. Steli, N. K. Sebbar, E. M. Essassi, M. Dahmani, Y. El Ouadi, A. Aouniti, B. El Mahi, B. Hammouti, *Der Pharma Chemica***, 2016**, 8(1), 248-256.
[30] H. Elmsellem, A. Elyoussfi, N. K. Sebbar, A. Dafali, K. Cherrak, H. Steli, E. M. Essassi, A. Aouniti and B. Hammouti, *Maghr, J. Pure & Appl. Sci*, **2015**, 1, 1-10.
[31] A. Elyoussfi, H. Elmsellem, A. Dafali, K. Cherrak, N. K. Sebbar, A. Zarrouk, E. M. Essassi, A. Aouniti, B. El Mahi and B. Hammouti, *Der Pharma Chemica*, **2015**, 7(10), 284-291.
[32] H. Elmsellem, H. Bendaha, A. Aouniti, A. Chetouani, M. Mimouni, A. Bouyanzer, *Mor. J. Chem*, **2014**, 2 (1), 1-9.
[33] N. K. Sebbar, H. Elmsellem, M. Boudalia, S. lahmidi, A. Belleaouchou , A. Guenbour, E. M. Essassi, H. Steli, A. Aouniti, *J. Mater. Environ. Sci*, **2015**, 6 (11), 3034-3044.
[34] H. Elmsellem, N. Basbas, A. Chetouani, A. Aouniti, S. Radi, M. Messali, B. Hammouti, *Portugaliae. Electrochimica. Acta*, **2014**, 2,77.
[35] H. Elmsellem, A. Elyoussfi, N. K. Sebbar, A. Dafali, K. Cherrak, H. Steli, E. M. Essassi, A. Aouniti and B. Hammouti. Maghr. J. Pure & Appl. Sci, **2015**, 1, 1-10.
[36] Y. El Ouadi, H. Elmsellem, M. El fal, N. K. Sebbar, A. Bouyanzer, R. Rmili, E. M. Essassi, B. El Mahi, L. Majidi & B. Hammouti, *Der Pharma Chemica*, **2016**, 8(1), 365-373.
[37] G. Avcı, *Mater. Chem. Phys*, **2008**,112, 234-238.
[38] H. Elmsellem, A. Aouniti,M. Khoutou, A. Chetouani, B. Hammouti, N. Benchat, R. Touzani and M. Elazzouzi, J. *Chem. Pharm. Res*, **2014**, 6, 1216.
[39] A.D. Becke, *Chem. Phys*, **1993**, 98, 5648.
[40] A.D. Becke, *Phys. Rev. A*, **1988,** 38, 3098.
[41] C. Lee, W. Yang, R.G. Parr, *Phys. Rev. B.*, **1988**, 37, 785.
[42] W. Wang, W.J. Mortier, *J. Am. Chem. Soc*., **1986,** 108, 5708.
[43] C.C. Zhan, J. A. Nichols, D.A. Dixon, *J.Phys.Chem. A*, **2003,**107, 4184.
[44] J.O.M. Bockris, B. Yang, *J. Electrochem. Soc*, **1991,**138, 2237.
[45]H. Elmsellem, K. Karrouchi, A. Aouniti, B. Hammouti, S. Radi, J. Taoufik, M. Ansar, M. Dahmani, H. Steli and B. El Mahi, *Der Pharma Chemica*, **2015**, 7(10),237-245.
[46] H. Elmsellem, A. Aouniti, Y. Toubi, H. Steli, M. Elazzouzi, S. Radi, B. Elmahi, Y. El Ouadi, A. Chetouani, B. Hammouti , *Der Pharma Chemica*, **2015**,7, 353-364.
[47] A. Aouniti, H. Elmsellem, S. Tighadouini, M. Elazzouzi, S. Radi, A. Chetouani, B. Hammouti, A. Zarrouk, *Journal of Taibah University for Science*, **2015**, http://dx.doi.org/10.1016/j.jtusci.2015.11.008.
[48] H. Elmsellem, N. Basbas, A. Chetouani, A. Aouniti, S. Radi, M. Messali, B. Hammouti, *Portugaliae. Electrochimica. Acta*, **2014**, 2, 77.
[49] H. Zarrok, A. Zarrouk, B. Hammouti, R. Salghi, C. Jama, F. Bentiss, *Corros. Sci*, **2012**, 64, 243.
[50] H. Elmsellem, A. Aouniti, Y. Toubi, H. Steli, M. Elazzouzi, S. Radi, B. Elmahi, Y. El Ouadi, A. Chetouani, B. Hammouti, *Der Pharma Chemica*, **2015**, 7, 353-364.
[51] H. Elmsellem, H. Nacer, F. Halaimia, A. Aouniti, I. Lakehal, A .Chetouani, S. S. Al-Deyab, I. Warad, R. Touzani, B. Hammouti, *Int. J. Electrochem. Sci*, **2014**, 9, 5328-5351.
[52] M. Sahin, S. Bilgic, H. Yılmaz, *Appl. Surf. Sci*, **2002,** 195, 1.
[53] M. Kissi, M. Bouklah, B. Hammouti, M. Benkaddour, *Appl. Surf. Sci*, **2006**, 252, 4190.
[54] E. Machnikova, K.H. Whitmire, N. Hackerman, Electrochim. Acta, **2008**, 53, 6024.
[55] O. Olivares, N.V. Likhanova, B. Gomez, J. Navarrete, M.E. Llanos-Serrano, E. Arce, J.M. Hallen, *Appl. Surf. Sci*, **2006**, 252, 2894.
[56] M. Lagrenee, B. Mernari, M. Bouanis, M. Traisnel, F. Bentiss, *Corros. Sci*, **2002**, 44 573.
[57] M. Hosseini, S.F.L. Mertens, M.R. Arshadi, *Corros. Sci*, **2003,** 45, 1473.
[58] H. Elmsellem, K. Karrouchi, A. Aouniti, B. Hammouti, S. Radi, J. Taoufik, M. Ansar, M. Dahmani, H. Steli and B. El Mahi, *Der Pharma Chemica*, **2015**, 7(10), 237-245.
[59] H. Elmsellem, T. Harit, A. Aouniti, F. Malek, A. Riahi, A. Chetouani , and B. Hammouti, *Protection of Metals and Physical Chemistry of Surfaces*, **2015**, 51(5), 873–884.

[60] N.O. Obi-Egbedi, I.B. Obot, M. I. El-Khaiary, S. A. Umoren, E. E. Ebenso, *Int. J. Electrochem. Sci.*, **2011**, 6, 5649.